

Tracking Small Low-Earth-Orbit Objects using a Fence-Type Radar

Thibaut Castaings¹, Benjamin Pannetier¹, Florent Muller¹, and Michèle Rombaut²

¹ONERA, Chemin de la Hunière, 91123 Palaiseau, France

²GIPSA-lab, 11 rue des Mathématiques, 38402 Saint Martin d'Hères, France

{thibaut.castaings, benjamin.pannetier, florent.muller}@onera.fr,
michele.rombaut@gipsa-lab.grenoble-inp.fr

Abstract

The use of a fence-type radar should enable the detection of smaller Low-Earth-Orbit objects (particularly debris) but involves Short Arcs (SA), which cannot be handled by existing tracking techniques. In this paper, we propose and investigate an approach based on an adapted Track-Oriented Multiple Hypothesis Tracking (TO-MHT) algorithm using new techniques able to associate SAs at one revolution of interval and to determine orbital states from such a pair of SAs.

Index Terms

space debris, short arcs, LEO, Multiple Hypothesis Tracking, MHT, tracking, orbit determination.

I. INTRODUCTION

Over time, space-based applications (such as space-based telecommunication, observation, navigation, etc.) have become essential for mankind to such an extent that their possible loss or even a possible inability to access space would imply severe aftermath [1][2][3]. As a consequence, the environment-related risks for space systems should be assessed and controlled. Following recent events, tracking space debris for collision avoidance has become a topic of great interest [4]. Still, the density of space debris is acceptable to operators in the sense of risk management in Mid-Earth-Orbit (MEO) and Geosynchronous-Earth-Orbit (GEO). This is why only the Low-Earth-Orbit (LEO) objects (of geodesic altitude lower than 2000Km) are within the scope of this paper. For the LEOs, radar-based surveillance sensors [5][6] use a large Field Of Regard (FOR), enabling the calculation of an orbital state at each pass of an object in order to associate passes at several revolutions of interval into tracks. As a consequence, the United States Space Surveillance Network is able to provide the United States Space Command (USSPACECOM) with the Space-Track Two-Lines Element (TLEs) catalog [7] containing the orbits of more than 15,000 objects with a diameter greater than 10cm, including the maneuvering satellites. Although the Space-Track TLE catalog contains a large majority of objects of diameter greater than 10cm, the estimated number of smaller objects is still greater [8][9] and has become a significant threat on the viability of space systems.

Aiming at tracking ever smaller and more numerous objects, with a higher accuracy, current sensors and methods are pushed to their limits. The best trade-off criterion for detecting smaller objects should be to increase the frequency of the emitted radio-wave [10]. To limit cost explosion, a reduced FOR, for instance a FOR of wide cross-elevation and narrow elevation (fence), is a possible option. This option is less costly but involves Short Arcs (SAs) from which an orbital state cannot be estimated, hardening the problem of associating the observations originated from the numerous LEO objects and filtering the generally high number of false alarms (FA) characterizing surveillance systems. However, an orbital state could be calculated from a set of SAs originated from the same object, but knowing the high number of LEO satellites – more than 11,000 objects of diameter greater than 10cm in the Space-Track catalog, more than 100,000 objects of diameter greater than 1cm and a high FA rate – testing all the possible combinations is prohibitive. Many methods have been developed for Multi-Target Tracking (MTT). The Track-Oriented Multiple Hypothesis Tracking algorithm (TO-MHT) [11][12][13] is often accepted as the preferred method to address difficult MTT problems. In a first time, the TO-MHT associates observations into tracks without requiring that the tracks do not share any observation, so that many observation-to-track association hypotheses are kept in memory until enough information is available to discriminate between them. Aside from the fact that the TO-MHT comprises several combinatory reducing steps, its ability to correctly associate observations into tracks strongly depends on the performance of a root, single-target tracking function (such as *e.g.* a Kalman filter [11]) providing state estimates and observation predictions. The observation predictions can be obtained from states estimates or using a prior knowledge of *e.g.* the maximal displacement from one scan to the other. However, several observations are required in most cases to compute a state estimate and the knowledge of the maximal displacement is efficient in a first time only if the target remains in the FOR from scan to scan.

To the purpose of tracking LEO objects using a fence-type radar, each object passing through the FOR produces a SA, *i.e.* only a couple of observations, with a low precision. As a consequence, although the observations originated from one penetration in the FOR may be associated into SAs with possibly a very low ambiguity, an orbital state cannot be estimated with sufficient precision to associate SAs at one or several revolutions of interval while avoiding a combinatorial explosion, taking into account that the generally high number of objects and FAs forbids the testing of all the combinations between the observations and FAs.

This paper addresses the problem of tracking the small LEO population from observations provided by a fence-type radar, with a particular focus on track initiation. To this purpose, we propose a method to limit the association possibilities of SAs at one revolution of interval and a method to initiate tracking from such a pair of SAs [14][15], in order to provide a TO-MHT with initialized tracks (*i.e.* tracks with state estimates).

This paper is organized as follows: we first briefly state the working hypotheses in Section II. The principle of the TO-MHT is recalled in Section III, as well as the principle of the tracking block in Section IV. Then, we discuss the choices made in the TO-MHT implementation regarding the features of the tracking block in Section V. The performance of tracking is assessed and discussed in Section VI and Section VII. Finally, a conclusion and leads of improvement are drawn in Section VIII.

II. POSITIONING

To this day, too few methods have been proposed to address the issue of track initiation for the tracking of small LEO objects. Based on [16], a technique called the Virtual Debris algorithm (VD) has been proposed and studied in [17][18][19], focusing on the tracking of the GEO population using optical sensors. Unfortunately, the experiments lead in these studies lack of ground-truth data for performance assessment and no experiment at all has been published concerning the possible extension of the VD to radar data, leaving the issue of tracking small LEO objects not addressed. The purpose of this work is to contribute to the development of a new data processing approach for the tracking – *i.e.* data association and state estimation – of the small, non-maneuvering (maneuvering objects being of a certain size, we assume that they can be handled by existing systems), LEO objects using a fence-type radar.

A. Dynamic Model

Predicting the position and velocity of an object taken from the Space-Track TLE catalog requires the use of a Simple General Perturbation (SGP) model. This model has been developed and described in [7] and predicts the effect of perturbations caused by the Earth's five first spherical harmonics and the atmospheric drag [7][20][21]. The orbital state components given in Table I are chosen in this study, the other parameters being set to a null value. The dependence

t	: Element Set Epoch,
n	: Mean Motion (revolutions/day), related to Semi-major axis a by Kepler's third law
e	: Eccentricity
i	: Orbit Inclination (degrees)
Ω	: Right Ascension of Ascending Node (degrees)
ω	: Argument of Perigee (degrees)
M	: Mean Anomaly (degrees), <i>i.e.</i> the position of the satellite on the orbit at time t
B^*	: Drag Term

Table I
DESCRIPTION OF THE CHOSEN ORBITAL STATE COMPONENTS.

of components n , e , i , Ω , ω and M on the element set epoch t will be omitted for the sake of clarity. Let \mathbf{X} refer to

the state vector $[n, e, i, \Omega, \omega, M, B^*]^T$ or $[n, e, i, \Omega, \omega, M]^T$, depending on the availability of B^* (the drag term B^* has an influence on a long time span and might be unavailable for short tracks), and $\mathbf{P}_{\mathbf{X}\mathbf{X}}$ its covariance matrix.

B. Sensor Characteristics

70 Forgetting technological constraints, some basic electromagnetics considerations [22] lead to the conclusion that the best trade-off criterion for detecting smaller objects should be to increase the frequency of the emitted radio-wave [10], which requires a reduced FOR to prevent cost explosion. To adhere to actual specifications of space surveillance systems currently being designed, we assume the following:

- The sensor is located in the northern hemisphere (latitude 45°).
- Its line of sight is oriented toward South with arbitrary-chosen 20° of elevation, with a wide cross-elevation (160°),
75 narrow elevation (2°) FOR.
- The FOR time of revisit is of 10s, *i.e.* the sensor produces one scan every 10s.
- It provides range ρ , azimuth θ and elevation ϕ measurements (pulsed monostatic), with a precision of $\sigma_\rho = 30m$ in range, $\sigma_\theta = 0.2^\circ$ in cross-elevation and $\sigma_\phi = 0.2^\circ$ in elevation.
- It has a false alarm rate of 1 FA/s.

Note that as the sensor provides 3D positioning measurements $\{\rho, \theta, \phi\}$, most of the processing may use a cartesian, Inertial Geocentric Frame of Reference (IGFR).

Let Z_k be the set of observations at scan k and m_k the number of observations at scan k . Let ρ_k^j , θ_k^j and ϕ_k^j denote the range, azimuth and elevation measurements of the j -th observation \mathbf{z}_k^j of scan k ; \mathbf{R}_k^j the covariance matrix of the measurement error; σ_ρ , σ_θ , σ_ϕ the uncertainties on range, azimuth, elevation such as (1).

$$\begin{aligned} Z_k &= \{\mathbf{z}_k^j\}_{j \in [1, m_k]} \\ \mathbf{z}_k^j &= [\rho_k^j, \theta_k^j, \phi_k^j]^T \\ \mathbf{R}_k^j &= \text{diag}(\sigma_\rho^2, \sigma_\theta^2, \sigma_\phi^2) \end{aligned} \quad (1)$$

Let $Z^{k,r}$ refer to the r -th sequence of p observations such as (2), where $k, k + i_1, \dots, k + i_p$ are the times of the observations. Note that the observations may be spaced by several revolutions.

$$Z^{k,r} = \{\mathbf{z}_k^{j_1}, \mathbf{z}_{k+i_1}^{j_2}, \dots, \mathbf{z}_{k+i_p}^{j_p}\} \quad (2)$$

80 C. Short Arcs

In the context of small object detection, an object going through the FOR produces an SA (*i.e.* one or two observations). We assume in this study that the observations originated from a single object during one pass through the FOR can be correctly associated using *e.g.* nearest neighbour approaches. Such considerations are out of the scope of this paper, so we focus in this study on the association of SAs. Let $A^{k,q}$ refer to the q -th SA containing the m successive observations $\mathbf{z}_k^{j_0}, \mathbf{z}_{k+1}^{j_1}, \dots, \mathbf{z}_{k+m-1}^{j_{m-1}}$ originated from a single pass of object through the FOR as given in (3), k being the instant of the latest observation. $Z^{k,r}$ may be expressed as (2) as well as (4), where p is the number of SAs it contains.

$$A^{k,q} = \{ \mathbf{z}_k^{j_0}, \mathbf{z}_{k+1}^{j_1}, \dots, \mathbf{z}_{k+m-1}^{j_{m-1}} \} \quad (3)$$

$$Z^{k,r} = \{ A^{k,q_1}, A^{k+i_2,q_2}, \dots, A^{k+i_p,q_p} \} \quad (4)$$

A set of SAs is required [15] to compute an orbital state with sufficient accuracy (*i.e.* to associate an observation with a track with little ambiguity) to track a LEO object, but as mentioned in the prequel, testing all the possible combinations results in a combinatorial explosion. The purpose of this work is to enable track initiation while avoiding such a combinatorial explosion, in order to find the most probable set of $\{Z^{k_i,r_i}\}_{i \in [1,I]}$ and associated orbital state estimates, I being the number of tracks in the most probable scenario.

III. PRINCIPLE OF THE TO-MHT ALGORITHM

The TO-MHT algorithm [12] aims at associating observations into tracks representing actual targets. In a first time, it forms tracks from new observations and existing tracks regardless to whether two tracks share an observation or not. Then, it deletes tracks according to some criteria before combining the surviving tracks into feasible hypotheses (hypotheses where tracks do not share any observation). After a hypothesis-level track deletion step, the remaining tracks are updated, merged and propagated to the time of the next scan. Figure 1 shows the high-level flowchart of the TO-MHT.

A. Track update and formation

When observations are associated to existing tracks at the previous iteration, the state estimates of the concerned tracks should first be updated with regard to the new observations they contain. Depending on the chosen tracking function, the Kalman filter update equations, a Least Squares (LS) minimization, a χ^2 minimization, or any suitable estimation technique can be used. As a consequence, an observation prediction function f_{SGP} (resulting from the SGP

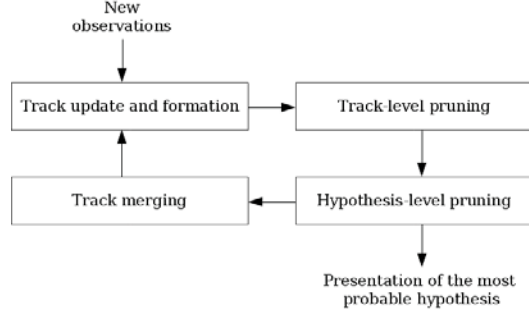


Figure 1. Global flowchart of a TO-MHT

model mentioned in Section II) can be used as shown in equation (5), where $\bar{\mathbf{z}}_{k+l}$ represents the predicted observation, k the time of the current scan and $k+l$ the instant of a future scan.

$$\bar{\mathbf{z}}_{k+l} = f_{SGP}(\mathbf{X}_k, l) \quad (5)$$

In order to assess the correlation of new observations with each track, a Validation Gate (VG) at future times can be computed using estimates of \mathbf{X} and $\mathbf{P}_{\mathbf{X}\mathbf{X}}$ through f_{SGP} using, *e.g.*, an Unscented Transform (UT). The principle of the UT lies in the computation and propagation of sigma-points [23] which have the same statistical features than the distribution defined by $\{\mathbf{X}, \mathbf{P}_{\mathbf{X}\mathbf{X}}\}$. The sigma-points propagated through f_{SGP} are used to estimate the distribution of the predicted observation $\{\bar{\mathbf{z}}, \mathbf{P}_{\bar{\mathbf{z}}\bar{\mathbf{z}}}\}$, where $\mathbf{P}_{\bar{\mathbf{z}}\bar{\mathbf{z}}}$ is the covariance matrix of $\bar{\mathbf{z}}$. A VG is obtained from such a distribution as the domain where the cumulative density function of $\{\bar{\mathbf{z}}, \mathbf{P}_{\bar{\mathbf{z}}\bar{\mathbf{z}}}\}$ is smaller than a predefined threshold γ . Usually and in this study, γ is set to 95%. Figure 2 shows an example of two existing tracks $Z^{k_1,1}$ and $Z^{k_2,2}$ at the instant k_3 of three new observations $\mathbf{z}_{k_3}^1$, $\mathbf{z}_{k_3}^2$ and $\mathbf{z}_{k_3}^3$. In this example, $\mathbf{z}_{k_3}^2$ would be associated to both $Z^{k_1,1}$ and $Z^{k_2,1}$. Besides, as the new observations may also represent new targets, new tracks would be formed from them as well.

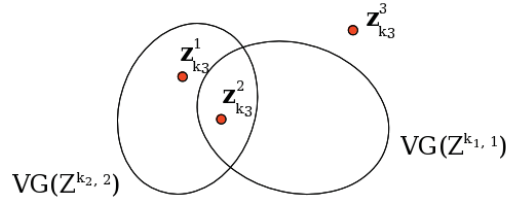


Figure 2. At time k_3 , new observations $\mathbf{z}_{k_3}^1$ and $\mathbf{z}_{k_3}^2$ fall in the VG of $Z^{k_1,1}$ or $Z^{k_2,1}$, $\mathbf{z}_{k_3}^3$ does not fall in any VG.

B. Track-level pruning

To prevent the number of hypotheses from exploding, the log-likelihood ratio $L^{k,r}$ of a track $Z^{k,r}$ is defined as a score in order to assess its quality, *i.e.* to delete or confirm it if necessary. Usually, this score is expressed as equation (6), where H_1 is the hypothesis “All the observations of $Z^{k,r}$ originated from the same object”, H_0 is the hypothesis “All the observations of $Z^{k,r}$ originated from FAs” and c is a constant. In other words, the Probability Density Function (PDF) of a predicted observation $\bar{\mathbf{z}}_{k+l}$ is evaluated with the actual observation \mathbf{z}_{k+l} for each observation the track contains in order to compute $p(Z^{k,r}|H_1)$, while the value of $p(Z^{k,r}|H_0)$ results from an assumed PDF of the FAs.

$$\begin{aligned} L^{k,r} &= \log \frac{p(Z^{k,r}|H_1)P_0(H_1)}{p(Z^{k,r}|H_0)P_0(H_0)} \\ &= \sum_{A^{k_i,q_i} \in Z^{k,r}} \log \frac{p(A^{k_i,q_i}|H_1)}{p(A^{k_i,q_i}|H_0)} + c \end{aligned} \quad (6)$$

As a consequence, scores associated to tracks vary as the tracks grow, until they reach a confirmation threshold T_2 or a deletion threshold T_1 , as shown in Figure 3. The values of these thresholds can be defined after the standard Sequential Probability Ratio Test (SPRT) formulation as in (7), where α and β are the probabilities of type I and type II errors.

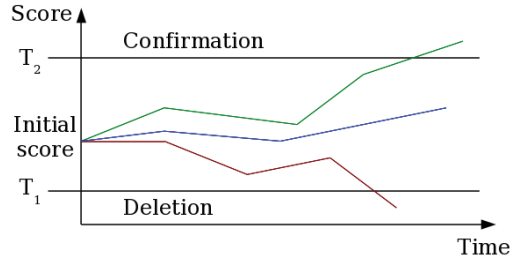


Figure 3. The track corresponding to the green curve is confirmed whereas the track corresponding to the red curve should be deleted. More information is required to confirm or to delete the track corresponding to the blue curve.

$$\begin{aligned} T_2 &= \log \frac{1-\alpha}{\beta} \\ T_1 &= \log \frac{\beta}{1-\alpha} \end{aligned} \quad (7)$$

The value of α should be chosen depending on the allowable probability that a false alarm generates a false track over a time lapse, whereas the value of β should be chosen depending on the capacity of the system to keep a large amount of hypotheses in memory.

C. Hypothesis-level pruning

After a track-level deletion step using the SPRT, the surviving tracks are separated into clusters [12][24] (sets of tracks bound by common observations) so that the association problem is divided into independant smaller problems.

For each cluster, the tracks are combined into J feasible hypotheses $\{h_j\}_{j \in [1, J]}$, *i.e.* into subsets so that two tracks cannot share directly any observation. In order to delete tracks with regard to global considerations, the “hypothesis-level” probability of each track in each cluster is computed from the likelihood of each track it contains, as expressed in (8), where $L^{k,r}$ denotes the likelihood of track $Z^{k,r}$, L_{h_j} the likelihood of hypothesis h_j , p_{h_j} the probability of hypothesis h_j , p_r the probability of track $Z^{k,r}$ at the hypothesis level and J the number of feasible hypotheses in the cluster.

$$\begin{aligned} L_{h_j} &= \sum_{Z^{k,r} \in h_j} L^{k,r} \\ p_{h_j} &= \frac{\exp(L_{h_j})}{1 + \sum_{i=1}^J \exp(L_{h_i})} \\ p_r &= \sum_{Z^{k,r} \in h_j} p_{h_j} \end{aligned} \quad (8)$$

The tracks of insufficient probability (below an user-defined threshold T_3) are deleted, whereas the surviving tracks are possibly merged before updating to avoid redundant computation.

110 D. Track merging

An MTT algorithm may generate redundant tracks, *i.e.* tracks which represent the same target, possibly implying unnecessary computation of state estimates. A first approach to handle this problem consists in defining merging criteria with regard to the common observations between tracks. For example, it is likely that two tracks represent the same target if they share a number of observations. Depending on the application, other features may be taken into account
 115 (*e.g.* the lengths of tracks). On the one hand, this approach lacks of a commonly-accepted similarity measure and requires empirical tuning but on the other hand, it does not require much computation nor the fine knowledge of a state. Another popular approach is presented in [25]. It relies on assessing the similarity between the states of two tracks using the state vector estimates and covariance matrices: a criterion may be defined on the statistical distance (*e.g.* Mahalanobis) or on each component, the choice of the criterion depending on the context.

120 If the merging criteria reach, then the track of maximum likelihood may be kept whereas the other are deleted, and its state may be updated regarding the states of the similar tracks. In this study, merging criteria regarding the number of common observations, the lengths of tracks and the statistical distance between two tracks are used.

Other approaches exist, such as *e.g.* mixture reduction algorithms [26] which consists in finding the minimal mixture representing the best the initial state mixture of a set of tracks.

IV. THE TRACKING BLOCK

Although the TO-MHT algorithm has been widely studied, the tracking block depends on the nature of the population to track. To the purpose of tracking the LEO population using sparse data, no tracking block has shown convincing performance to this day in the task of track initiation, as mentioned earlier in Section II. As a matter of fact, our previous work presented in [14] and [15] focuses on the design of a new technique to initiate tracks in such a context. The purpose of this paper, we recall, is to study the feasibility of an MTT algorithm – a TO-MHT appears to be a relevant choice – using this technique. The major issue tackled in [14] and [15] is that each new SA may originate from a new target whereas no state can be estimated to correlate future SAs and decide whether or not this hypothesis is likely (due to the lack of information contained in a single SA).

At first, SAs at one revolution of interval are correlated, starting from a set of behavioural features [14] extracted from a simulation using a Space-Track TLE catalog. Then, starting from two SAs at one revolution of interval, an approach to estimate initial orbits of six orbital elements with sufficient precision to track objects is proposed [15]. The performance of the track initiation block resulting from the chaining of the methods (as shown in Figure 4) is assessed as a component of a TO-MHT. The principles of these techniques are recalled in this section.

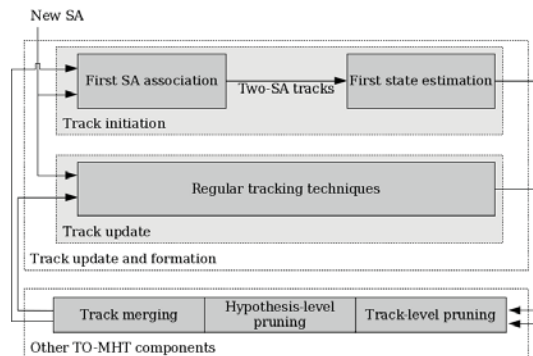


Figure 4. Integration of the track initiation function comprising a first-association step ([14]) and a first state estimation step ([15]) in a TO-MHT using regular tracking techniques.

140 A. Association of SAs at one revolution of interval

This method correlates SAs using information extracted from the simulation (dynamic observer) of a set-up {sensor, existing catalog} described in Section II in order to compute a spatio-temporal gate and to score the generated association hypotheses. The principle of this method lies in the use of the motion pseudo-periodicity: from a revolution to the other, the LEO objects take “neighbouring” positions in an IGFR. In a first time, we define in the sequel a set of features, namely the time lapse before reappearance d_T , the difference of radius d_ρ and the “longitudinal distance” $d_{\rho\theta}$ in an

IGFR, able to define such a neighbourhood.

As input data, the sensor features (namely location and FOR shape) as well as a set of orbits of interest (*e.g.* the Space-Track TLE catalog), must be provided as shown on Figure 5. For the sake of clarity, only the key steps of this technique are presented in the following. The reader would refer to [14] for more detailed explanations. Using a

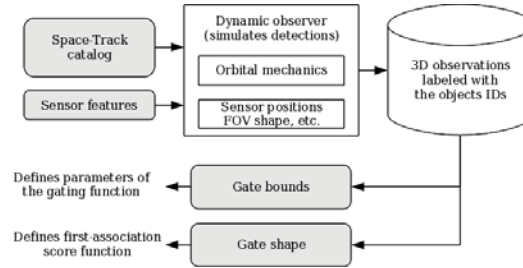


Figure 5. A good sample of the LEO population, such as a Space-Track catalog, as well as the sensor features must be provided to characterize the detection of objects bound to the laws of orbital mechanics.

dynamic observer as described in Figure 5 enables to extract useful information without handling orbital mechanics – orbital mechanics leading so far to unsolved problems for tracking space objects using a fence-type radar – in order to reduce the number of possible associations. This procedure is done offline, only its output is used in the real-time processing.

1) *Spatial gating*: We define a spatial gate around an SA using the two distances d_ρ and $d_{\rho\theta}$ defined so that: if $Z^{k,r}$ is a track containing an SA A^{k_1,q_1} of cardinal m_1 , and A^{k_2,q_2} is a candidate SA of cardinal m_2 for association, then the distances $d_\rho(A^{k_1,q_1}, A^{k_2,q_2})$ and $d_{\rho\theta}(A^{k_1,q_1}, A^{k_2,q_2})$ are given by (9), where $\rho^{A^{k,q,j}}$ and $\theta^{A^{k,q,j}}$ are respectively the radius and longitude of observation j of $A^{k,q}$ in a spherical IGFR.

$$\begin{aligned}
 d_\rho(A^{k_1,q_1}, A^{k_2,q_2}) &= \frac{1}{m_1} \sum_{j=1}^{m_1} \rho^{A^{k_1,q_1,j}} \\
 &\quad - \frac{1}{m_2} \sum_{j=1}^{m_2} \rho^{A^{k_2,q_2,j}} \\
 d_{\rho\theta}(A^{k_1,q_1}, A^{k_2,q_2}) &= \frac{1}{m_1} \sum_{j=1}^{m_1} \rho^{A^{k_1,q_1,j}} \theta^{A^{k_1,q_1,j}} \\
 &\quad - \frac{1}{m_2} \sum_{j=1}^{m_2} \rho^{A^{k_2,q_2,j}} \theta^{A^{k_2,q_2,j}}
 \end{aligned} \tag{9}$$

The distances d_ρ and $d_{\rho\theta}$ appear to be uncorrelated, which is an advantage since, as it is shown in the sequel, their heights are of a different order of magnitude if the pair of SAs originated from the same object. The dynamic observer is then used to find out what maximal values d_ρ and $d_{\rho\theta}$ may take if the pair of SAs originates from the same object (hypothesis H_1), enabling to build a VG along those dimensions.

The distance values are relatively low on the axis of radial difference d_ρ and relatively high on the axis of longitudinal

distance $d_{\rho\theta}$. Besides, the law of probabilities $p(d_\rho(A^{k_1,q_1}, A^{k_2,q_2})|H_1)$ and $p(d_{\rho\theta}(A^{k_1,q_1}, A^{k_2,q_2})|H_1)$ do not correlate
 160 with the mean radius of the SAs. As a consequence, fixed thresholds are chosen to limit their supports to reasonable bounds.

2) *Time gating*: The probability density of the time lapse d_T before reappearance of an object knowing its mean geocentric radius $\bar{\rho}^{A^{k,q}}$ over an SA $A^{k,q}$ should be estimated. For that purpose, we use the dynamic observer to build the distribution of pairs of SAs originated from the same object in the plane $(\bar{\rho}, d_T)$ and deduce the probability density of
 165 $p(d_T(A^{k_1,q_1}, A^{k_2,q_2})|\bar{\rho} = \bar{\rho}^{A^{k_1,q_1}}, H_1)$, resulting in a VG along the time dimension after applying a suitable threshold.

3) *Score function of an association*: In order to assess the quality of an association, *i.e.* to delete or confirm a track comprising a pair of SAs at one revolution of interval, a likelihood ratio computed using the densities of $d_T|H_1$, $d_\rho|H_1$ and $d_{\rho\theta}|H_1$ evaluated with $(A^{k_1,q_1}, A^{k_2,q_2})$ can be taken as an initial score $L_0^{k,r}$, such as shown in (11), where d is the function defined as (10), $V_{T,\rho,\rho\theta}$ is the volume of the gate formed by d_T , d_ρ and $d_{\rho\theta}$, and N the number of SAs falling in it.

$$d: \mathfrak{R}^{3 \times m_1} \times \mathfrak{R}^{3 \times m_2} \mapsto \mathfrak{R}^3$$

$$A^{k_1,q_1}, A^{k_2,q_2} \mapsto \begin{pmatrix} d_T(A^{k_1,q_1}, A^{k_2,q_2}) \\ d_\rho(A^{k_1,q_1}, A^{k_2,q_2}) \\ d_{\rho\theta}(A^{k_1,q_1}, A^{k_2,q_2}) \end{pmatrix} \quad (10)$$

$$L_0^{k,r} = \log \frac{p(d(A^{k_1,q_1}, A^{k_2,q_2})|H_1)}{p(d(A^{k_1,q_1}, A^{k_2,q_2})|H_0)}$$

$$= \log(p(d_T(A^{k_1,q_1}, A^{k_2,q_2})|\bar{\rho} = \bar{\rho}^{A^{k_1,q_1}}, H_1)$$

$$\times p(d_\rho(A^{k_1,q_1}, A^{k_2,q_2})|H_1) \quad (11)$$

$$\times p(d_{\rho\theta}(A^{k_1,q_1}, A^{k_2,q_2})|H_1)$$

$$\times \frac{V_{T,\rho,\rho\theta}}{N})$$

This score expression is derived from (6) in the case of the association of observations at one revolution of interval, and can be compared to the thresholds T_1 and T_2 defined in (7).

B. State estimation from two-SA tracks

Statement 1. *The track contains observations spaced enough to make the system observable, i.e. it contains observations*
 170 *forming an angle θ greater than an empirically-chosen value $\theta_{observable}$ in an IGFR.*

To initiate the tracking of an object, its state \mathbf{X} should be computed for each pair of correlated SAs resulting from the first SA association technique recalled in the prequel, so the unlikely hypotheses are deleted when sufficient information is available. However, the observation noise and the proximity of observations forbids the use of well-known Lambert's

methods [27][15], and empirically, the system becomes observable when Statement 1 is true, *i.e.* at least one more SA should be associated for the state to be estimated with sufficient precision to enable tracking with little ambiguity. As a consequence, a truncated state \mathbf{X}_4 should be estimated at first.

1) *Overview of the state estimation step:* Let \mathbf{X}_4 refer to the state vector $[n, i, \Omega, M]^T$ and $\mathbf{P}_{\mathbf{X}\mathbf{X},4}$ to its covariance matrix. A Gauss-Newton algorithm (GN) [28] may be used to estimate the state and an Unscented Transform (UT) [23] may be used to associate new SAs to a track. As a consequence, the method follows three steps [15], starting from a pair of SAs at one revolution of interval:

- Determine a sufficient approximation of \mathbf{X}_4 geometrically with a covariance matrix $\mathbf{P}_{\mathbf{X}\mathbf{X},4}$.
- Associate an SA of the opposite node for Statement 1 to become true, using an UT.
- Solve a least squares problem using a GN algorithm to estimate \mathbf{X} and $\mathbf{P}_{\mathbf{X}\mathbf{X}}$.

The estimation through the GN algorithm and the association using an UT can be used for track update as well, such as shown on Figure 6. Values for the eccentricity e and the argument of perigee ω are retrieved while solving the least

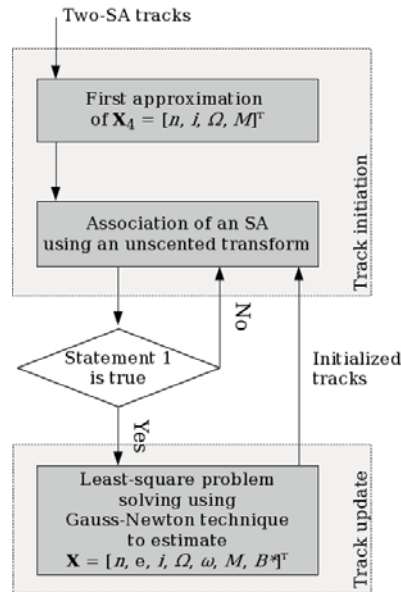


Figure 6. The track initiation step follows three steps.

185

squares problem in the third step, enabling the application of regular tracking techniques afterwards.

2) *Estimation of \mathbf{X}_4 :* Starting from two SAs at one orbit of interval, the state $\mathbf{X}_4 = [n, i, \Omega, M]^T$ may be retrieved geometrically, assuming that its drift is negligible over one revolution. Let \mathbf{z}_{k_1} and \mathbf{z}_{k_2} be the position-vectors of an observation taken from the first SA and of an observation taken from the second SA in such a IGFR, τ the time lapse between those observations, and α the geocentric angle between \mathbf{z}_{k_1} and \mathbf{z}_{k_2} . In this case, the object travelled over an

190

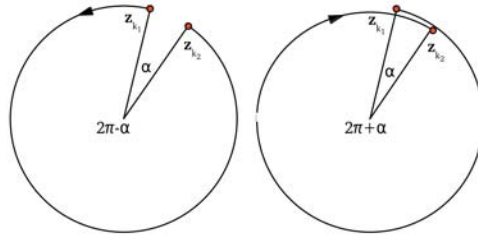


Figure 7. The object travelled less than one revolution (left). The object travelled more than one revolution (right).

angle $2\pi \pm \alpha$ as shown on Figure 7. A large majority of LEO objects being of very low eccentricities, it is often possible to use Kepler's third law to discriminate between the two obtained values of n . If the angle α is too small to make such a choice, then both cases should be kept in memory until more SAs are added to the track. Fair approximations of n , i , Ω and M are given by (12), where \mathbf{p} is the cross product of \mathbf{z}_{k_1} and \mathbf{z}_{k_2} .

$$\begin{aligned}
 n &\simeq \frac{2\pi \pm \alpha}{\tau} \\
 i &\simeq \arccos \frac{\mathbf{p} \cdot \mathbf{u}_Z}{\|\mathbf{p}\|} \\
 \text{if } \mathbf{p} \cdot \mathbf{u}_Y \geq 0, \Omega &\simeq \frac{\pi}{2} + \arccos \frac{\mathbf{p} \cdot \mathbf{u}_X}{\|\mathbf{p} \cdot \mathbf{u}_X + \mathbf{p} \cdot \mathbf{u}_Y\|} \\
 \text{else } \Omega &\simeq \frac{\pi}{2} - \arccos \frac{\mathbf{p} \cdot \mathbf{u}_X}{\|\mathbf{p} \cdot \mathbf{u}_X + \mathbf{p} \cdot \mathbf{u}_Y\|} \\
 \text{if } \mathbf{z}_{k_1} \cdot \mathbf{u}_Z \geq 0, M &\simeq \arccos \frac{\cos \Omega \mathbf{z}_{k_1} \cdot \mathbf{u}_X + \sin \Omega \mathbf{z}_{k_1} \cdot \mathbf{u}_Y}{\|\mathbf{z}_{k_1}\|} \\
 \text{else } M &\simeq -\arccos \frac{\cos \Omega \mathbf{z}_{k_1} \cdot \mathbf{u}_X + \sin \Omega \mathbf{z}_{k_1} \cdot \mathbf{u}_Y}{\|\mathbf{z}_{k_1}\|}
 \end{aligned} \tag{12}$$

195 Computing several values of n , i , Ω and M using a set of randomly chosen values of \mathbf{z}_{k_1} and \mathbf{z}_{k_2} in the error volumes of the observations enables the calculation of a covariance matrix $\mathbf{P}_{\mathbf{X}\mathbf{X},4}$. The bias induced by the ignorance of e and ω should be compensated by the addition to $\mathbf{P}_{\mathbf{X}\mathbf{X},4}$ of a diagonal matrix $\mathbf{D}_{\mathbf{X}\mathbf{X},4}$ with well-chosen coefficients. Regular filtering techniques such as the UT may be used to associate new SAs from the resulting couple $\{\mathbf{X}_4, \mathbf{P}_{\mathbf{X}\mathbf{X},4}\}$ until Statement 1 becomes true.

200

V. ON THE EFFICIENCY OF THE DELETION STEPS

The combinatorial complexity involved in tracking the LEO population may be limited by the use of a gating function of sufficient precision and a score-function providing sufficient separability between correct and wrong tracks. As opposed to the gating function, the score-function relies on an MTT algorithm to delete tracks. As a consequence, analyzing the behaviour of the score-function is of interest in order to implement a suitable MTT algorithm. Figure 205 8 shows the evolution of the score of correct tracks against the number of SAs they contain. This experiment has

been made using the Space-Track TLE catalog and a SGP propagator on a simulation of observations from the sensor described in Section II over three days.

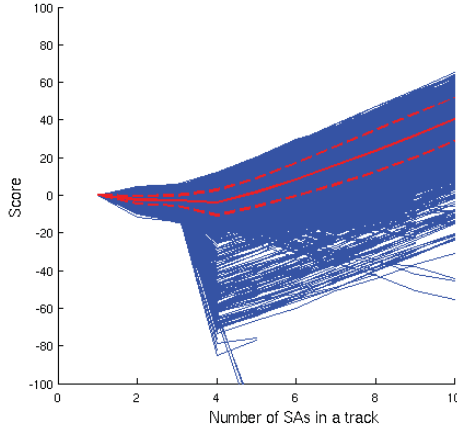


Figure 8. Score against length of the track. The blue lines plot the 20,724 track scores, their mean is plotted with a red, bold line and their standard-deviation with a red, bold, dashed line.

The score stays about zero until Statement 1 becomes true (3.74 SAs on the mean) and increases significantly afterwards. This behaviour of the score-function is relevant since making Statement 1 true corresponds to making the system observable. In other words, the object is in a lock-on step as long as Statement 1 is not true. As a consequence, the tracks which survived the track-level deletion step have similar scores, so they get low hypothesis-level probabilities and may get mistakenly deleted. For instance, consider a cluster containing two tracks $Z^{k_1,1}$ and $Z^{k_2,2}$ of scores 3 and -2 , respectively. The use of (8) yields hypothesis-level probabilities of 0.95 and 0.006, respectively, possibly resulting in the deletion of $Z^{k_2,2}$ although it may be true. Moreover, any track of low score (Statement 1 is false) sharing an SA with a track of high score (Statement 1 is true) yields categorical probabilities (either close to 1 or 0) resulting in the deletion of any not confirmed track sharing an SA with a confirmed track, which can be done an easier way. As a consequence, we decided not to use such hypothesis-level deletion methods and to rely on other combinatory-reducing techniques such as track merging.

Figure 9 shows the distribution of the number of correlated SAs using \mathbf{X} , *i.e.* after Statement 1 became true. At this stage, the objects are tracked with little ambiguity (1.10 SA per VG on the mean), suggesting that both a method using a common observation ratio and a method correlating orbital states should perform well as merging techniques.

VI. PERFORMANCE

The adapted TO-MHT algorithm has been implemented. In the section, its performance is assessed.

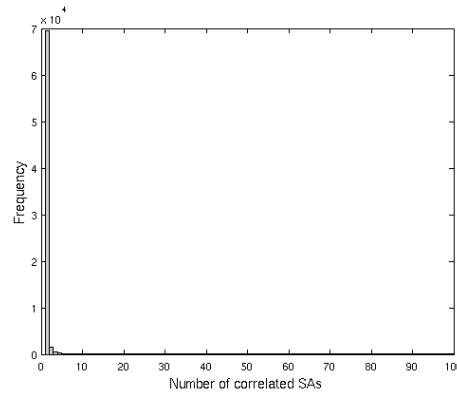


Figure 9. Distribution (Mean = 1.10) of the number of SAs correlated to a track using the orbital state \mathbf{X} and $\mathbf{P}_{\mathbf{X}\mathbf{X}}$, *i.e.* after Statement 1 became true.

A. Experimental conditions

225 To assess the performance of this implementation of the TO-MHT for tracking small LEO objects, we have run a simulation of the observations of 547 objects by the sensor configuration described in Section II, over 10 days. The objects are chosen in the Space-Track catalog so that they all pass in the FOR on a 15-minute time span (*i.e.* they actually pass each other), making a hard problem to solve. FAs are randomly added to each scan where actual objects appear: 265,410 FAs are added to the 26,541 scans resulting from the simulation (*i.e.* 1 FA/s according to Section II),
 230 making the detection density realistic while avoiding the processing of clutter-only scans.

B. Criteria of performance

In this case, mainly three key performance criteria appeared to be important to us:

Criterion 1. *The ratio of the number of objects the algorithm can track with no redundancy and a high degree of certainty (non-redundant confirmed tracks) over the number of simulated objects.*

235 **Criterion 2.** *The ratio of the size of memory used to store the confirmed tracks over the size of memory used to store all the tracks.*

Criterion 3. *The ratio of the number of redundant confirmed tracks over the total number of confirmed tracks.*

Calculating those criteria enables to assess the number of objects the algorithm would be able to track (Criterion 1, which should be as high as possible), as well as its ability to delete tracks efficiently (Criterion 2, which should be as high as possible). The ability of the algorithm to fuse redundant tracks reflects on Criterion 3, which should be as low
 240 as possible.

C. Setting of the algorithm

The implementation of the TO-MHT involves many parameters which should be set to proper values. Most of them, such as the probabilities of type I and type II errors α and β related to the thresholds T_1 and T_2 defined by (7), may be easily set according to the user requirements and to the peculiarities of the problem to solve. However, some parameters involved in the new techniques carried out in this work have a significant impact on the performance of the overall algorithm and require arduous tuning. These are:

- the coefficients of the diagonal matrix $\mathbf{D}_{\mathbf{X}\mathbf{X},4} = \text{diag}(\kappa_1, \kappa_2, \kappa_3, \kappa_4)$ reflecting the uncertainty induced by the assumption of circular orbits made in IV-B2.
- the least angle $\theta_{observable}$ between two associated observations in a IGFR making Statement 1 true.
- the threshold $\theta_{statistical\ merge}$ related to the statistical distance computed to assess the similarity between two tracks during the merging step.

Table II lists the main parameter values retained for the experiments lead in this study. Note that the size (scale factor)

Parameter	Value
κ_1 (associated to n)	8×10^{-9} rad/s
κ_2 (associated to i)	8×10^{-3} rad
κ_3 (associated to Ω)	8×10^{-3} rad
κ_4 (associated to M)	8×10^{-9} rad
$\theta_{observable}$	1.2 rad
$\theta_{statistical\ merge}$	93%
α	1.157×10^{-6}
β	10^{-3}

Table II
MAIN PARAMETER VALUES RETAINED FOR EXPERIMENTS.

and shape (relative values of the coefficients) of the 4-D ellipsoid defined by $\mathbf{D}_{\mathbf{X}\mathbf{X},4}$ have been independently optimized.

D. Results

Figure 10, Figure 11 and Figure 12 show the evolutions of Criterion 1, Criterion 2 and Criterion 3 over the simulated time.

Criterion 1 converges to 87.6% at the end of the simulation although it does not increase at every scan. Criterion 2 increases over the 10 simulated days until it reaches about 34.3%, whereas Criterion 3 remains at less than 1% during most of the simulated time.

For illustrative purpose, Appendix shows the estimated trajectory (yellow) of a LEO object (altitude of approximately

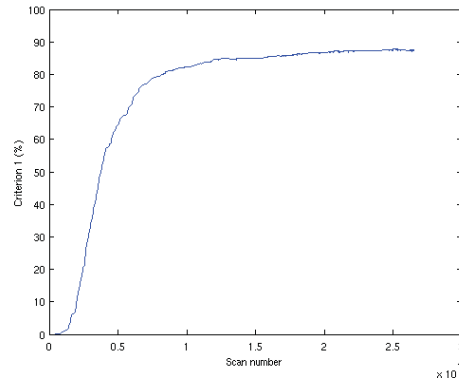


Figure 10. Evolution of the ratio of objects the algorithm can track with a high degree of certainty over all the simulated objects (Criterion 1) over the simulated time.

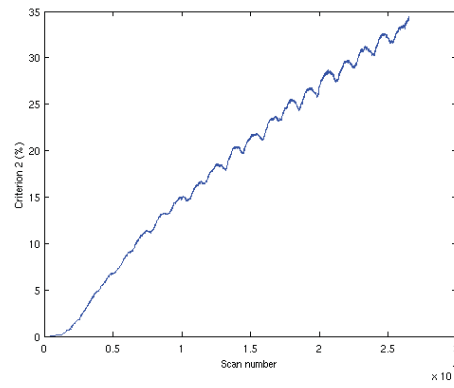


Figure 11. Evolution of the ratio of the size of memory used to store the confirmed tracks over the size of memory used to store all the tracks (Criterion 2) over the simulated time.

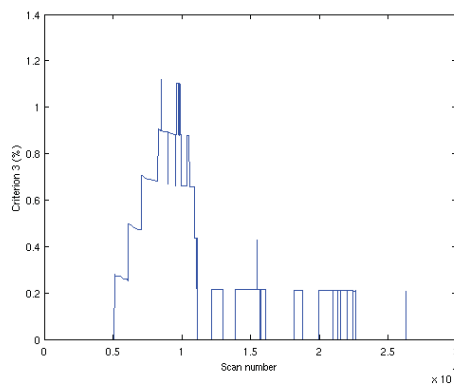


Figure 12. Evolution of the ratio of the number of redundant confirmed tracks over the total number of confirmed tracks (Criterion 3) over the simulated time.

900Km) using a track resulting from the use of our algorithm on a simple scenario (29 objects and 20,420FAs). The red dots represent the observations made on the scans containing the elements of the track; the cyan dots show the location of the sensor and the contour of the intersection of the FOR with the sphere of altitude 900Km.

VII. DISCUSSION AND LEADS OF IMPROVEMENT

The evolutions of Criterion 2 and Criterion 3 shown on Figure 11 and Figure 12 appear quite satisfactory to us. Indeed, Criterion 2 is constantly increasing up to about 34.3%, *i.e.* more and more memory is used for tracks which represent actual objects. Moreover, Criterion 3 remains at a low value (less than 1%), proving that the redundant tracks are properly merged. Besides, Criterion 1 increases quickly after a short simulated time until it converges to a fair value of 87.6%, which shows that the algorithm is able to track a large majority of objects but with a few losses.

Criterion 1 being an end point criterion (the system aims at tracking as many objects as possible) as opposed to Criterion 2 and Criterion 3, it is important to understand why Criterion 1 does not reach a higher convergence value. This may be explained by two reasons: firstly, some objects may be lost as other objects are tracked; secondly, some objects with peculiar orbital states would not be tracked.

The loss of an object may happen due to:

- a divergence or convergence to a wrong value during the estimation step using a GN method.
- a bad association, *i.e.* an observation originated from another object or an FA induces the best score increment.
- a wrong decision during track merging.

An object may not be tracked because:

- the object rarely passes through the FOR at one revolution of interval.
- the object passes through the FOR at one revolution of interval, but the pair of SAs it generates is rejected.
- the truncated state \mathbf{X}_4 computed from a correct pair of SAs originated from the object does not correlate with a correct third SA so that Statement 1 is true.

The experiments showed that about 8.6% of the observed objects could not be tracked whereas 3.8% of the objects were tracked then lost using our techniques, on a 10-day time span. These numbers might be decreased by a finer tuning of the parameters, especially of the thresholds related to the gating and the merging of tracks (in this study, these thresholds are set to 95% and 93%, respectively). Criterion 3 being very low, strengthening the merging threshold should improve Criterion 1 at an acceptable cost on Criterion 3.

In [14], experiments over a period of 30 days show that 99.8% of the LEO objects contained in the Space-Track TLE catalog pass through the FOR at one revolution of interval at least one time and that 37.4% of the SAs from the same

object are observed at one revolution of interval on the mean. As a consequence, the first reason mentioned to explain why an object may not be tracked should be dispelled.

Aside from that, the threshold and the smoothing applied on the distributions resulting from the method proposed in [14] might not be optimal, so that some objects might not be handled. Indeed, in our experiments, about 10% of the pairs of SAs generated by the dynamical observer are cropped before smoothing, *i.e.* only 90% of these pairs of SAs are used to estimate the densities of d_ρ , $d_{\rho\theta}$ and d_T , possibly resulting in a too high rejection rate.

As for the third reason, using the truncated state \mathbf{X}_4 assumes that most of the objects are of very low eccentricities, *i.e.* that most LEO objects are on a near circular orbit, which is a reasonable assumption, since 95% of the LEO objects contained in the Space-Track catalog have an eccentricity smaller than 0.05. However, the set of the objects which could not be tracked should be studied in order to determine whether or not specific orbit parameter values are more frequent comparing to statistical features over the set of the tracked LEO objects.

The short analysis stated hereinbefore supports that the most promising leads of improvement regarding Criterion 1 should be to optimally estimate the probability densities used in the first association of SAs (see Section IV-A and [14]) and to improve the first state estimation and association step until Statement 1 is true. However, a more complete analysis should be done in order to confirm these leads. Besides, a few low-level blocks (such as *e.g.* the GN block) should be robustified in order to avoid as many losses as possible.

VIII. CONCLUSION

In this paper, we have presented the principles of new techniques as well as their performance in an MTT frame. We have highlighted the main adaptations a TO-MHT should undergo in order to take advantage of the new tracking block that constitutes the chaining of these techniques. Although the new processing of which we attempt to prove the feasibility is not utterly mastered at the moment, its current performance appeared to be more than promising for the task of tracking small LEO objects using a fence-type radar. Indeed, a large majority of the simulated population was tracked using our approach, with very low redundancy after convergence. Finally, a short analysis has been drawn in order to identify the key factors to focus on in order to improve the functioning of the algorithm. This analysis shows that the three main leads of improvement concern the estimation of the probability densities used in the first association step, the first state estimation and association step until Statement 1 is true, and a few low-level blocks which should be robustified. As a consequence, the performance and its analysis tend to support the feasibility of the approach we propose in this paper and provide leads to investigate in future works.

REFERENCES

- 320 [1] N. H. Fischer and R. C. Reynolds, "Threat of space debris," *Military Communications Conference, IEEE*, 1984.
- [2] O. of Science en Technological Policy, "Interagency report on orbital debris," in *The National Science and Technology Council, Committee on Transportation Research and Development*, 1995.
- [3] E. Fletcher, "Space situational awareness: An analysis of threats, consequences and future solutions for europe's security, safety and prosperity.," tech. rep., European Space Agency, 2010.
- 325 [4] E. Hody, S. Bertrand, F. Muller, P. Brudieu, and F. Alby, "Analysis of the residual risk of lethal collisions for leo satellites due to non catalogued objects," *62nd International Astronautical Congress, Cape Town, South Africa*, 2011.
- [5] P. W. J. Schumacher, "Us naval space surveillance upgrade program 1999-2003," in *7th US/Russian Space Surveillance Workshop Proceedings, Naval Postgraduate School, CA*, 2007.
- [6] T. Michal, J. P. Eglizeaud, and J. Bouchard, "Graves: the new french system for space surveillance," in *Proceedings of the 4th European Conference on Space Debris (ESA SP-587)*, 2005.
- 330 [7] F. R. Hoots and R. L. Roehrich, "Models for propagation of norad element sets, spacetrack report no. 3," tech. rep., US Air Force, 1980.
- [8] D. Kessler, "Collisional cascading: The limits of population growth in low earth orbit," *Advances in Space Research*, 1991.
- [9] E. G. Stansbery, "Growth in the number of ssn tracked orbital objects," *55th International Astronautical Congress, Vancouver, Canada*, 2004.
- [10] E. F. Knott, J. F. Shaeffer, and M. T. Tuley, *Radar Cross Section*. Artech House Radar Library, 1985.
- 335 [11] S. S. Blackman, "Multiple hypothesis tracking for multiple target tracking," *Aerospace and Electronic Systems Magazine, IEEE*, 2003.
- [12] S. S. Blackman and R. Popoli, *Design and Analysis of Modern Tracking Systems*. Artech House Radar Library, 1999.
- [13] Y. Bar-Shalom, *Multitarget-Multisensor Tracking: Principle and Techniques*. Burlington, MA: Academic Press, 1995.
- [14] T. Castaings, B. Pannetier, F. Muller, and M. Rombaut, "Sparse data association for low earth orbit tracking," in *Aerospace Conference, IEEE*, 2012.
- 340 [15] T. Castaings, F. Muller, B. Pannetier, and M. Rombaut, "Track initiation using sparse radar data for low earth orbit objects," in *63rd International Astronautical Congress, Naples, Italy*, 2012.
- [16] A. Milani, G. Gronchi, M. Vitturi, and Z. Knezevic, "Orbit determination with very short arcs. i admissible regions," *Celestial Mechanics and Dynamical Astronomy*, 2004.
- [17] G. Tommei, A. Milani, and A. Rossi, "Orbit determination of space debris: admissible regions," *Celestial Mechanics and Dynamical Astronomy*, 2007.
- 345 [18] D. Farnocchia, G. Tommei, A. Milani, and A. Rossi, "Innovative methods of correlation and orbit determination for space debris," *Celestial Mechanics and Dynamical Astronomy*, 2010.
- [19] A. Milani, G. Tommei, D. Farnocchia, A. Rossi, T. Schildknecht, and R. Jehn, "Orbit determination of space objects based on sparse optical data," *Monthly Notices of Royal Astronomical Society*, 2011.
- 350 [20] D. A. Vallado, P. Crawford, R. Hujsak, and T. S. Kelso, "Revisiting spacetrack report no. 3," tech. rep., American Institute of Aeronautics and Astronautics, 2006.
- [21] M. H. Lane, P. M. Fitzpatrick, and J. J. Murphy, "On the representation of air density in satellite deceleration equations by power functions with integral exponents," tech. rep., Air Force Systems Command, 1962.
- [22] D. Deirmendjian, "Electromagnetic scattering on spherical polydispersions," tech. rep., RAND Corporation, 1969.
- 355 [23] S. J. Julier, J. K. Uhlmann, and H. F. Durrant-Whyte, "A new approach for filtering nonlinear systems," in *Proceedings of the American Control Conference, Seattle, Washington, pages 1628-1632*, 1995.
- [24] S. Baase, *Computer Algorithms: Introduction to Design and Analysis*. Reading, MA: Addison-Wesley, 1978.

- [25] S. S. Blackman, *Multiple Target Tracking with Radar Applications*. Artech House, 1986.
- [26] L. Y. Pao, "Multisensor multitarget mixture reduction algorithms for tracking," *Journal of Guidance, Control and Dynamics*, 1994.
- 360 [27] L. A. Loechler, *An Elegant Lambert Algorithm for Multiple Revolution Orbits*. Massachusetts Institute of Technology, Department of Aeronautics and Astronautics, 1988.
- [28] K. Madsen, H. Bruun, and O. Tingleff, "Methods for non-linear least squares problems," tech. rep., Technical University of Denmark, 1999.

APPENDIX: ILLUSTRATION

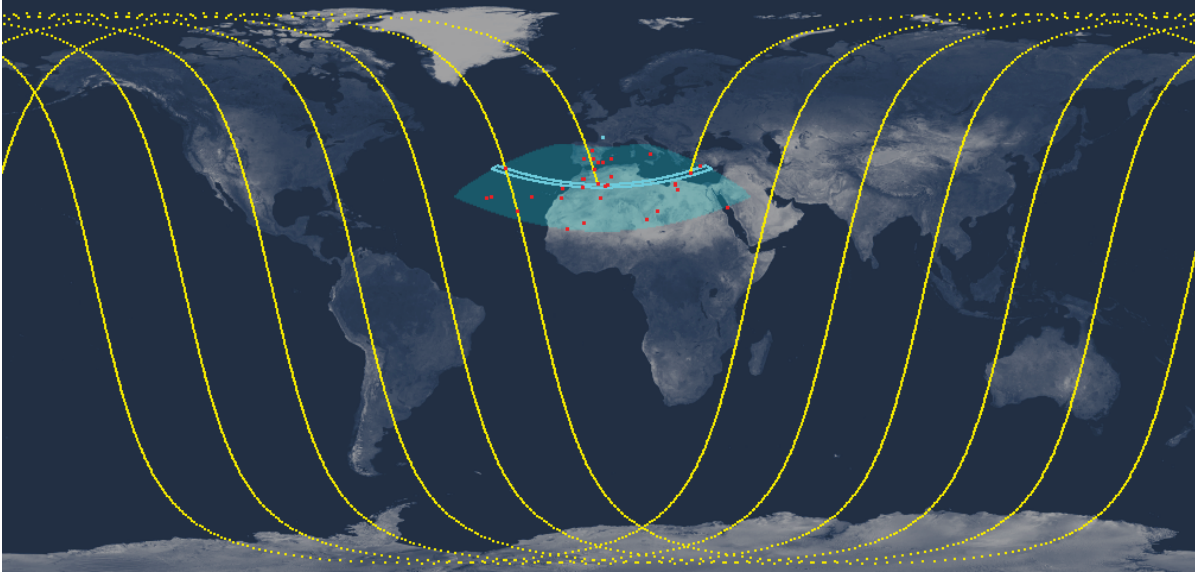


Figure 13. Estimated trajectory (yellow) of a LEO object (altitude of approximately 900Km) using a track resulting from the use of our algorithm on a simple scenario (29 objects and 20,420FAs). The red dots represent the observations made on the scans containing the elements of the track. The cyan dots show the location of the sensor and the contour of the intersection of the FOR with the sphere of altitude 900Km. The dark cyan area represents the FOR at all the altitudes it covers. The elements of the track are the observations seen on the trajectory and in the FOR contour.